

Spontaneous trimerization in a bilinear-biquadratic $S = 1$ zig-zag chain

Philippe Corboz,¹ Andreas M. Läuchli,² Keisuke Totsuka,³ and Hirokazu Tsunetsugu⁴

¹*Institut für Theoretische Physik, ETH Zürich, CH-8093 Zürich, Switzerland*

²*Institut Romand de Recherche Numérique en Physique des Matériaux (IRRMA), CH-1015 Lausanne, Switzerland*

³*Yukawa Institute for Theoretical Physics, Kyoto University,
Kitashirakawa Oiwake-Cho, Kyoto 606-8502, Japan*

⁴*Institute for Solid State Physics, University of Tokyo, Kashiwa, Chiba 277-8581, Japan*

(Dated: February 1, 2008)

Recent theoretical studies raised the possibility of a realization of spin nematic states in the $S = 1$ triangular lattice compound NiGa_2S_4 . We study the bilinear-biquadratic spin 1 chain in a zig-zag geometry by means of the density matrix renormalization group method and exact diagonalization. We present the phase diagram focusing on antiferromagnetic interactions. Adjacent to the known Haldane-double Haldane and the extended critical phase with dominant spin nematic correlations we find a *trimerized* phase with a nonvanishing energy gap. We discuss results for different order parameters, energy gaps, correlation functions, and the central charge, and make connection to field theoretical predictions for the phase diagram.

PACS numbers: 75.10.Jm, 75.10.Pq, 75.40.Cx, 75.40.Mg

Introduction — Quantum spin systems have provided a very wide playground for the quest of novel quantum orders, and the short catalog includes Haldane gap, dimer order, chiral order and others. Recently the discovery of spin liquid like behavior in the spin-1 triangular magnet NiGa_2S_4 [1] has stimulated increasing interests in another type of quantum order: spin nematic order. This is the long range order of quadrupole moments of local spins, in contrast to dipole moment order parameter in conventional magnetic long range orders. In a spin nematic ordered phase, although spins show no static moment, spin rotation symmetry is spontaneously broken due to anisotropic spin fluctuations. For $S=1$ spin operators, anisotropic spin fluctuations still have uniaxial symmetry, and this symmetry axis is called director, in analogy to a liquid crystal. Ferro and antiferro spin nematic orders were independently proposed by different groups as an explanation for the unusual low-temperature properties of NiGa_2S_4 [2, 3, 4]. In particular, the antiferro spin nematic order is possible to match the triangular lattice structure without any frustration, and the ground state is unique aside from degeneracy due to global spin rotation. Although it remains open if antiferro spin nematic order is realized in this material, it is interesting and also important to investigate further this state and obtain a better understanding. To this end, we shall study a one-dimensional analog with the same three sublattice structure, a zig-zag chain.

Model — The Hamiltonian of the bilinear-biquadratic (BLBQ) spin 1 zig-zag chain is given by

$$H = J_1 \sum_i \cos \theta (\mathbf{S}_i \cdot \mathbf{S}_{i+1}) + \sin \theta (\mathbf{S}_i \cdot \mathbf{S}_{i+1})^2 + J_2 \sum_i \cos \theta (\mathbf{S}_i \cdot \mathbf{S}_{i+2}) + \sin \theta (\mathbf{S}_i \cdot \mathbf{S}_{i+2})^2. \quad (1)$$

\mathbf{S}_i 's are spin 1 operators and θ parametrizes the strength

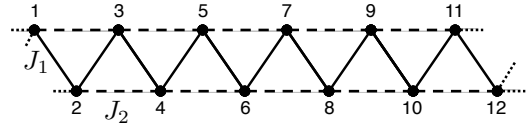


FIG. 1: Zig-zag geometry of the model with J_1 (J_2) the nearest (next nearest) neighbor coupling strength.

of bilinear and biquadratic coupling. For $\theta = 0$ ($\theta = \pi/2$) the biquadratic terms (bilinear terms) vanish. For $\theta = \pi/4$ the Hamiltonian exhibits $\text{SU}(3)$ spin symmetry. J_1 and J_2 are the nearest and next nearest neighbor coupling strengths, respectively. The model is best visualized in a zig-zag geometry where the J_1 bonds couple two chains and the J_2 bonds are located along the chains (Fig. 1). We concentrate on antiferromagnetic interactions on all bonds with $0 \leq \theta \leq \pi/2$ and $J_1, J_2 \geq 0$. By setting $\theta = 0$ the model reduces to the $J_1 - J_2$ spin 1 chain which exhibits a first order transition between two distinct topological orders [5]. The Haldane phase for $J_2/J_1 < \alpha_t \approx 0.775$, which also contains the well studied spin 1 chain for $J_2 = 0$, is characterized by a finite string order parameter (SOP). The ground state is a valence bond solid (VBS) where each site consists of two spin 1/2 forming a triplet and two spin 1/2 on neighboring sites couple to a singlet. The transition into the double Haldane (DH) phase corresponds to a decoupling of the VBS string into two intertwined substrings, where each string exhibits string order [5], leading to a finite *double* string order parameter (DSOP).

The line $J_2/J_1 = 0$ corresponds to the BLBQ chain studied, e.g., in [6]. The gapped Haldane phase (including the Affleck-Kennedy-Lieb-Tasaki (AKLT) point for $\tan \theta = 1/3$) ends at the $\text{SU}(3)$ symmetric point $\theta = \pi/4$ (exactly solvable Uimin-Lai-Sutherland model) where a second order phase transition of Berezinskii-Kosterlitz-

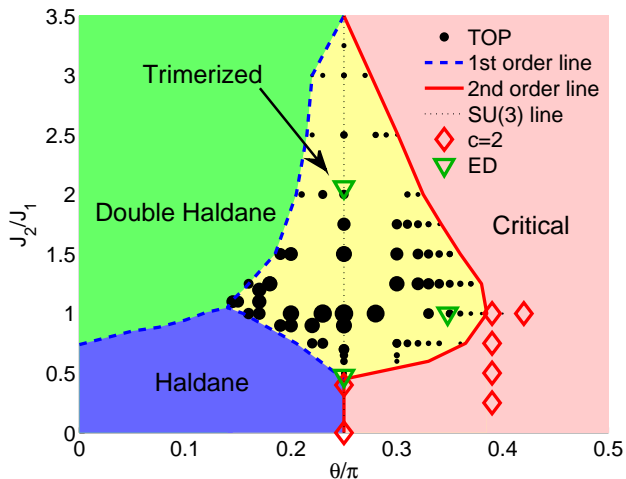


FIG. 2: (Color online) The phase diagram of the spin 1 BLBQ zig-zag chain. The area of the black dots in the trimerized phase scales with the magnitude of the trimer order parameter. We verified that the central charge is 2 in the critical phase for several points (red diamonds). The green triangles mark the phase boundary of the trimerized phase obtained from a level spectroscopy analysis from the ED data.

Thouless (BKT) type occurs [7]. Thus there is an exponentially slow opening of the gap on the Haldane side. For $\pi/4 \leq \theta < \pi/2$ one finds an extended critical phase with soft modes at $k = 0, \pm 2\pi/3$ and central charge $c = 2$. The dominant correlations in this phase away from the SU(3) point are quadrupolar (spin nematic) [6, 7].

Numerical simulations — The numerical results have been obtained by the density matrix renormalization group (DMRG) [8, 9] method and exact diagonalization (ED). For the DMRG calculations we used up to $m = 2000$ states with typically 6 sweeps and system sizes with open boundary conditions up to $L = 300$ sites. Quantities of interest are extrapolated in m and if needed also for $L \rightarrow \infty$. Error bars are estimated from the convergence behavior in m . With ED we considered systems with periodic boundary conditions up to $L = 21$.

The overall phase diagram — Figure 2 summarizes the phase diagram of the Hamiltonian (1) obtained by DMRG and ED simulations. We reproduced the results for the phases on the axes: Haldane, the DH, and the extended critical phase with $c = 2$. All these phases extend into the plane. Interestingly they all touch the dominant phase in the center, a gapped trimerized phase, which will be discussed below.

The Haldane - double Haldane transition [5] point extends as a first order line in the parameter space which terminates upon touching the boundary of the trimerized phase. We confirmed the first order nature of the transitions by calculating the SOP and DSOP along several cuts for fixed θ and varying J_2/J_1 .

Trimerized phase — The most exciting feature of the phase diagram is the gapped, trimerized phase, where

three neighboring spins couple predominantly to a singlet. The trimer ground state is threefold degenerate and breaks translational invariance. This phase – including the frustration process leading to it – is reminiscent of the dimerized phase of the J_1 - J_2 spin 1/2 chain for $J_2/J_1 \geq 0.2411$ [10].

Initially a massive trimerized phase for the spin 1 Heisenberg chain ($J_2/J_1 = 0$) for $\pi/4 < \theta < \pi/2$ was put forward [11, 12], but later works [6, 7, 13, 14, 15, 16] showed that the region remains massless and has dominant nematic correlations. In our model the additional next nearest neighbor coupling J_2 allows us to stabilize the trimerized state.

In previous work [17, 18] parent Hamiltonians have been constructed using complicated four site interactions, which exhibit exact trimer ground states (in Ref. [19] yet a different kind of trimerized state was constructed). We now have found a trimerized phase that is stable in a finite region of the parameter space of a much simpler and possibly realistic spin Hamiltonian. We expect our model (1) to be related to these parent Hamiltonians in Refs. [17] and [18] in the same spirit as the Heisenberg spin 1 chain is related to the AKLT model.

One of the most direct indications for a trimerized phase is the period 3 in the local bond energies (insets of Fig. 3). This pattern is formed because the two bonds belonging to a trimer have a lower energy than the bonds connecting two trimers. We determine this oscillation amplitude of the local bond energies in the middle of the chain for different system sizes L and extrapolate it to $L \rightarrow \infty$. In the Haldane (respectively DH) phase the amplitude vanishes exponentially with L . In the critical region the amplitude extrapolates to zero with a power law. But in the trimerized phase the extrapolation of the oscillation amplitude clearly yields a finite value, which we call the trimer order parameter (TOP) (see Fig. 3).

The magnitude of the TOP in the trimerized phase is proportional to the area of the black dots in Fig. 2. On

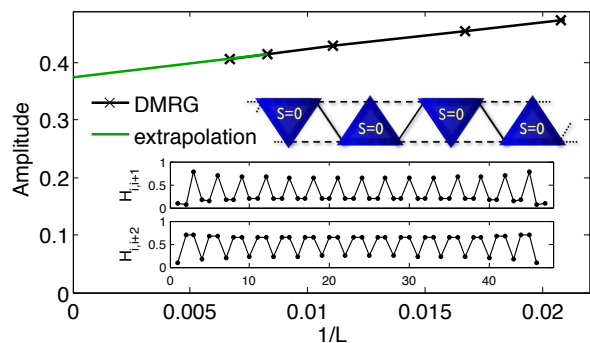


FIG. 3: (Color online) Extrapolation of the bond energy oscillation amplitude in the middle of the chain leading to a finite trimer order parameter in the trimerized phase ($\theta = 0.28\pi$, $J_2/J_1=1$). Inset: The local bond energies form a pattern of period 3 ($L = 48$ in this example).

the SU(3) line DMRG predicts that the trimerized phase sets in at $J_2/J_1 \approx 0.45$ and ends at ≈ 3.5 . We used a level spectroscopy analysis of the ED data to complement the results (green triangles in Fig. 2). This technique has been successfully applied in the case of the spin 1/2 chain to locate the transition point into the dimerized phase [10]. ED yields a consistent result with DMRG for the lower boundary of the trimerized phase, but it suggests a substantially smaller value for the upper boundary. This mismatch stems partly from strong finite size effects on the location of the level crossings (which are much stronger than in the spin 1/2 case). We observe that the ED phase boundary shifts to slightly larger J_2 values upon taking bigger system sizes into account, approaching somewhat the DMRG results. A different source of error is the rather slow convergence of DMRG in m in or close to a critical phase, especially for large J_2/J_1 . The important result, however, which we get from both methods is the *finite* extent of the trimerized phase on the J_2/J_1 axis, in contrast to the spin 1/2 case where the dimerized phase extends to infinity. We comment on a possible explanation in the field theory section below.

Figure 4 shows the finite spin gap in the trimerized phase, $\Delta E = E_0(1) - E_0(0)$ where $E_0(S^z)$ is the ground state energy in the S^z sector. On the SU(3) line the lowest excitation is eightfold degenerate (i.e. spin and quadrupolar excitations are symmetry related on this line). Away from the SU(3) line the lowest excitations have $S_{tot} = 1$ for $\theta < \pi/4$ and $S_{tot} = 2$ for $\theta > \pi/4$. According to the analysis of Ref. 18, the nature of excitations in the trimerized phases are gapped, deconfined domain walls, very similar to the deconfined spinons of the spontaneously dimerized phase of the frustrated $S = 1/2$ spin chain.

The BKT transition line lies on the SU(3) line except for $0.45 \leq J_2/J_1 \leq 3.5$ where it follows the right boundary of the trimerized phase. Field theory predicts that the transition line separating the Haldane (respectively DH) phase from the trimerized phase is of first order (see below). We confirmed this numerically from a non-vanishing spin gap and a non diverging spin-spin correla-

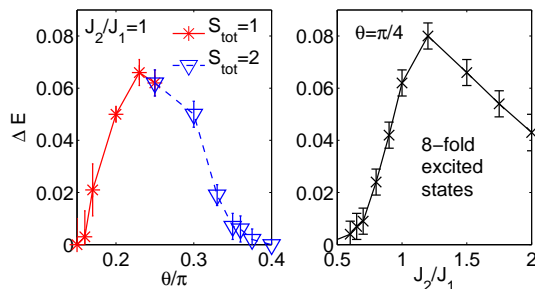


FIG. 4: (Color online) Energy gaps of spin excitations along cuts in the parameter space with $J_2/J_1 = 1$ (left-hand side) and $\theta = \pi/4$ (right-hand side).

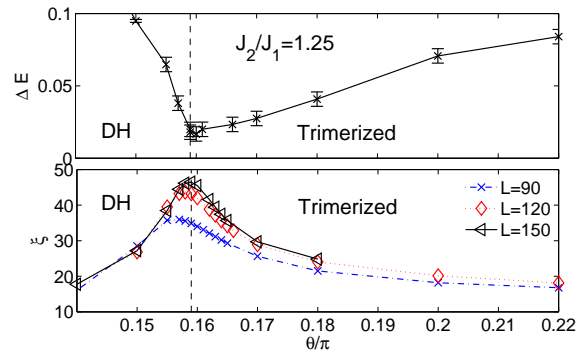


FIG. 5: (Color online) Energy gap between the ground state of singlet and triplet sector (upper plot) and spin correlation length (lower plot) for different system sizes for fixed $J_2/J_1 = 1.25$. The finite energy gap at the transition and the weak size dependence of the correlation length indicate a first order phase transition. The correlation length was obtained by a fit to the exponential decay of the spin-spin correlations.

tion length across the transition for $J_2/J_1 = 1.25$ (Fig. 5). For $J_2/J_1 = 0.75$ we cannot completely rule out a vanishing gap as it is rather small at the transition. Another indication for the first order nature is the jump of the TOP at the phase boundary, in contrast to the exponential suppression of the TOP towards the critical phase.

Critical phase — We have determined the value of the central charge numerically from the entanglement entropy for different points in the critical phase (red diamonds in Fig. 2), and all the values agree with $c = 2$ (to within 5%), corresponding to a level-1 SU(3) Wess-Zumino-Witten (WZW) model [7]. We made use of the universal scaling behavior of the entanglement entropy for conformally invariant one-dimensional quantum systems [20] of the form $S(x, L) = \frac{c}{6} \ln \left[\frac{2L}{\pi} \sin \left(\frac{\pi x}{L} \right) \right] + \text{const}$, where $S(x)$ is the von Neumann entropy of the reduced density matrix $\hat{\rho}(x)$ of a subsystem starting at the open boundary of length x embedded in a system of length L , and c is the central charge. In the critical phase the spin and quadrupolar correlation functions are expected to decay as a power law with distance x with an exponent $\eta = 4/3$ and multiplicative logarithmic corrections [7] $\sim \cos(2\pi x/3)(\ln x)^\sigma/x^\eta$, which suppress the spin ($\sigma = -2$) and enhance the quadrupolar ($\sigma = 2$) correlations, such that the latter are dominant (Fig. 6), similar to the single chain case [6].

Field theoretical considerations — As is discussed in [7, 21], the low-energy effective Hamiltonian for the model (1) around the point $J_2 = 0$, $\theta = \pi/4$ is the level-1 SU(3) WZW model perturbed by marginally irrelevant current-current interactions:

$$\mathcal{H}_{\text{WZW}} + v g_1 \int dx \sum_{A \in \text{SO}(3)} J_L^A J_R^A + v g_2 \int dx \sum_{A \in \text{others}} J_L^A J_R^A, \quad (2)$$

where the first summation is over the SO(3)-subset of the SU(3)-currents $J_{L,R}^A$. The choice $g_1 = g_2 = g$ recovers

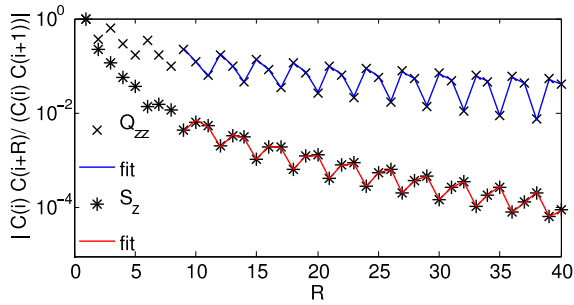


FIG. 6: (Color online) Spin (stars) and quadrupolar (crosses) correlation functions (normalized) for $\theta = 0.42\pi$, $J_2 = 0.25$. The two solid lines are fits to the functional form predicted by field theory. Logarithmic corrections to the power law lead to dominant quadrupolar correlations.

SU(3) symmetry and the integrable model ($J_2 = 0$, $\theta = \pi/4$) corresponds to $g < 0$.

At the leading order, the effect of $J_2(>0)$ (with $\theta = \pi/4$ fixed) may be taken into account by increasing $g(=g_1=g_2)$ in Eq. (2). At some critical value of J_2 , g changes its sign to positive and the system flows into a massive phase with three degenerate ground states [22]. The model (2) has another massive phase characterized by the asymptotic trajectory $g_1 = -g_2$, which has a unique (Haldane) ground state and is separated from the trimerized one by a first-order transition [22]. The Y-shaped boundaries (among *trimerized*, *Haldane* and *critical*) and other qualitative features in the lower portion of Fig. 2 are consistent with what is predicted by the model (2). The appearance of the gapless phase in the large- J_2 region ($J_2/J_1 \gtrsim 3.5$), as revealed by DMRG and ED may be understood as follows. Let us start with two weakly coupled BLBQ chains. From the field-theoretical viewpoint, the ordinary two-leg ladder and the zig-zag chain should behave similarly in the decoupled chain limit; both systems will flow toward a strong-coupling limit upon switching on the interchain coupling J_1 . From the standard expansion with respect to the strongly coupled rungs, we know that the strong-coupling phase of the ordinary two-leg BLBQ ladder ($\theta > \pi/4$) is critical (as in the $S = 1/2$ three-leg ladder). Therefore we may expect the same critical behavior in the zig-zag ladder as well at least for sufficiently large J_2/J_1 .

Conclusions — We have presented a study of a spin 1 generalization of the famous $J_1 - J_2$ $S=1/2$ model, motivated by recent proposals for spin nematic ground states in a spin 1 triangular lattice [2, 3, 4]. The phase diagram generalizes the well-known spin fluid-dimerized transition to a (nematic) spin fluid to trimerized transition in the level-1 SU(3) WZW universality class. We further explored the phase diagram in the vicinity of this transition, revealing a realization of the gapped sector of the Andrei-Destri model. Coming from the limit of two decoupled BLBQ chains the interchain interaction is rele-

vant and drives a crossover to gapless single-chain behavior, in contrast to the $S=1/2$ case, where the marginal interaction lets the system flow to a dimerized strong coupling state.

As a perspective we believe that the SU(N) $J_1 - J_2$ model contains a general mechanism where the critical state realized for the J_1 model flows towards a N -merized gapped state when the ratio J_2/J_1 is beyond a certain critical value. Another interesting point is the possibility of stabilizing trimerized phases in two dimensional lattices, possibly in a $J_1 - J_2$ BLBQ model on the triangular lattice. Furthermore in the light of the present study, where we revealed dominant quadrupolar correlations in the vicinity of the SU(3) line, it will be interesting to explore whether other spin nematic or spin-multipolar phases [23] remain to be uncovered close to SU(N) regions in higher spin antiferromagnets.

PC acknowledges inspiring discussions with M. Matsumoto, M. Troyer, and U. Schollwöck, and ETH Zurich for allocation of CPU time on the Gonzales cluster. AML acknowledges the support of the Swiss National Fund and thanks F. Mila and K. Penc for work on related topics. The ED simulations have been enabled by the allocation of computing time at CSCS in Manno. HT was supported by a Grant-in-Aid for Scientific Research (Grants No. 17071011 and No. 16540313), and also by the Next Generation Super Computing Project, Nanoscience Program, from the MEXT of Japan.

-
- [1] S. Nakatsuji, Y. Nambu, H. Tonomura, O. Sakai, S. Jonas, C. Broholm, H. Tsunetsugu, Y. Qiu, and Y. Maeno, *Science* **309**, 1697 (2005).
 - [2] H. Tsunetsugu and M. Arikawa, *J. Phys. Soc. Jpn.* **75**, 3701 (2006).
 - [3] A. Läuchli, F. Mila, and K. Penc, *Phys. Rev. Lett.* **97**, 087205 (2006).
 - [4] S. Bhattacharjee, V. B. Shenoy, and T. Senthil, *Phys. Rev. B* **74**, 092406 (2006).
 - [5] A. K. Kolezhuk and U. Schollwöck, *Phys. Rev. B* **65**, 100401(R) (2002).
 - [6] A. Läuchli, G. Schmid, and S. Trebst, *Phys. Rev. B* **74**, 144426 (2006).
 - [7] C. Itoi and M. H. Kato, *Phys. Rev. B* **55**, 8295 (1997).
 - [8] S. R. White, *Phys. Rev. Lett.* **69**, 2863 (1992).
 - [9] U. Schollwöck, *Rev. Mod. Phys.* **77**, 259 (2005).
 - [10] K. Okamoto and K. Nomura, *Phys. Lett. A* **169**, 433 (1992).
 - [11] Y. Xian, *J. Phys.: Condens. Matter* **5**, 7489 (1993).
 - [12] K. Nomura and S. Takada, *J. Phys. Soc. Jpn.* **60**, 389 (1991).
 - [13] G. Fáth and J. Sólyom, *Phys. Rev. B* **44**, 11836 (1991).
 - [14] P. Reed, *J. Phys. A* **27**, L69 (1994).
 - [15] R. J. Bursill, T. Xiang, and G. A. Gehring, *J. Phys. A* **28**, 2109 (1995).
 - [16] A. Schmitt, K.-H. Mütter, M. Karbach, Y. Yu, and G. Müller, *Phys. Rev. B* **58**, 5498 (1998).

- [17] K. Penc, unpublished (2002).
- [18] M. Greiter, S. Rachel, and D. Schuricht, Phys. Rev. B **75**, 060401(R) (2007).
- [19] J. Sólyom and J. Zittartz, Europhys. Lett. **50**, 389 (2000).
- [20] P. Calabrese and J. Cardy, J. Stat. Mech.: Theory Exp. (2004) P06002.
- [21] I. Affleck, Nucl. Phys. B **305**, 582 (1988).
- [22] P. Lecheminant and K. Totsuka, J. Stat. Mech.: Theory Exp. (2006) L12001.
- [23] T. Momoi, P. Sindzingre, and N. Shannon, Phys. Rev. Lett. **97**, 257204 (2006).